Engineering Journal issn: 0125-8281

Article

Development of Lightweight Concrete Interlocking Block Panel with Water Treatment Sludge and Expanded Metal Ferrocement

Rattawit Amornpunyapat[1], Phaiboon Panyakapo[1,*], and Mallika Panyakapo[2]

1 Department of Civil Engineering and Town Development, School of Engineering, Sripatum University, Bangkok 10900, Thailand
2 Department of Environmental Science, Faculty of Science, Silpakorn Univerity, Nakornpathom 73000, Thailand
*E-mail: phaiboon.pa@spu.ac.th (Corresponding author)

Abstract. An innovative lightweight concrete interlocking block panel was developed to improve the lateral resistance of the infilled frame with green construction material. The water treatment sludge obtained from Bang Khen water treatment plants was employed to replace the fine aggregate. The lightweight concrete interlocking block panel was strengthened with ferrocement technique and expanded metal sheet. Three sets of the strengthened block panels with various sizes of expanded mental were investigated: concrete block panel, interlocking block panel with thin bed adhesive mortar, interlocking block panel with thick bed cement mortar. The concrete with mixed proportion of cement, sand, water, foaming agent, and sludge of 1:0.70:0.60:0.006:0.30 by weight was suitable for producing the lightweight concrete block according to the Thai Industrial Standard. The compressive strength test of masonry prisms and the diagonal tension (shear) test were conducted for the three sets of the strengthened block panels. The test results reveal that the interlocking block was superior to the conventional concrete block in terms of strength and ductility capacity due to the effect of interlocking between the block. The shear key with thick bed cement mortar is more effective than the thin bed adhesive mortar typically used in the construction of lightweight concrete.

Keywords: Lightweight concrete, interlocking block, water treatment sludge, expanded metal.

ENGINEERING JOURNAL Volume 25 Issue 1
Received 6 July 2020
Accepted 25 November 2020
Published 31 January 2021
Online at https://engj.org/
DOI:10.4186/ej.2021.25.1.81

DOI:10.4186/ej.2021.25.1.81

1. Introduction

The great earthquake event which occurred in Chiang Rai, the Northern part of Thailand on May 5, 2014 with 6.3 Richter caused an important effect on many existing buildings. Particularly, the brick infilled panels were damaged due to the lateral force of the infill-frame interaction effect. Typically, the brick infill panels are not considered to resist the lateral force in the design of buildings. The compressive strength and the diagonal tension strength of the conventional brick panel are relatively low, therefore, causing damage to the infilled frame. One of the commonly used techniques of seismic strengthening of brick panel is ferrocement with welded wire mesh. S. B. Kadam et al. [1] investigated the shear and ductility capacity of 12 sets of brick masonry panel strengthened with ferrocement under diagonal compession test. Various types of wire mesh wrapping and anchorages were employed to investigate the bond strength of weld wire mesh and masonry. Significant enhancement was observed for the shear strength and ductility capacity due to the effect of reinforcement ratio of ferrocement. The effects of strengthening brick infill panel on the lateral resistance of infilled frame under cyclic loading were conducted by A. Leeanansaksiri et al. [2]. The brick panel was strengthened with ferrocement and expanded metal. The retrofit frame not only enhanced the strength but also the stiffness and the energy dissipation capacity. However, the corner compression failure of the wall occurred due to high concentration of the applied lateral load. It was recommended to protect against corner crushing of the brick panel. Further research was also conducted to remedy this problem by S. Longthong et al. [3]. The corner crushing was successfully protected by the technique of steel plate attaching at the wall corner.

To improve the strength of infill panel, interlocking concrete block with shear key at the interface of each block is an alternative construction material to protect against sliding shear failure. M. Ali et al. [4] investigated the shear strength of the interlocking panel mixed with coconut fiber under in-plane and out-of-plane monotonic loading. The out-of-plane shear strength was 25% higher than the in-plane shear. Z. Tang et al. [5] also investigated the shear strength of mortar-free interlocking panel with coconut fiber. The in-plane shear strength was slightly increased under dynamic loading. P. Joyklad et al. [6] studied the mechanical properties of cement clay interlocking brick with various types of mixed proportion. The cement content was more effective than sand and fly ash contents. The axial compression and diagonal compression tests of cement clay interlocking brick walls were also investigated by P. Joyklad and Q. Hussain [7, 8]. The effects of grouting and steel reinforcement enhanced the compressive strength, shear strength and ductility capacity of the wall. However, the self-weight of concrete block occasionally cause difficulty in the construction hence the lightweight concrete block becomes more competitive. For example, an application of waste marble powder as a lightweight aggregate was incorporated into the interlocking block by Q. Afzal et al. [9]. The compressive strength was satisfied with the code requirement for 10% addition of waste. Therefore, as an alternative, the reuse of the waste material for producing the lightweight concrete interlocking block with green construction material is a promising approach.

The water treatment sludge is the waste from the water treatment process. The Bang Khen water treatment plant has encountered with large quantity of sludge of 75-105 tons per day leftover for disposal. The disposal expense of the sludge was over 350,000 USD per year. Therefore, the utilization of sludge not only increases the waste value but also reduce the disposal cost. It was reported that the sludge from Bang Khen water treatment plant was composed of SiO_2, Al_2O_3, Fe_2O_3, in a proportion of 67%, 23%, 6%, respectively [10, 11]. The content of organic matter was relatively low. The physical properties of sludge can be classified as clayey sand with a specific gravity of 2.67-2.68 which can be used as fine aggregate for the replacement of sand. The effect of sand replacement by the water treatment sludge on the compressive strength of concrete has been studied by R.K. Gomes et al. [12]. The wet sludge was employed as a partial replacement of sand ranging from 0, 5, 7, 10 percentage by weight of fine aggregate. The compressive strength decreased for the increase of sludge content. Nevertheless, it was reported by Y. Liu et al. [13] that the compressive strength could be increased at the low sludge content of 5% replacement of sand. However, these researches are based on the wet raw sludge. The dry aluminium-based sludge has been used as a partial replacement of cement content for the pozzolanic addition [14]. The dry-based sludge content was varied between 10% and 30% of cement by weight. The compressive strength was decreased by 30% and 45%, respectively. Similar results were also investigated [15-18]. The application of water treatment sludge as the lightweight aggregate was employed by sintering process to obtain the particle density ranging from 0.65-2.05 g/cm^3 [19]. Both strength and density decreased with the increase of w/c ratio. The alum-based sludge and sawdust were also used as lightweight aggregate for concrete composite [20, 21]. The density of the product increased with the thermal conductivity. The concrete composite can be applied for nonstructural lightweight concrete.

In this study, the water treatment sludge was employed as a partial replacement of fine aggregate. The mix proportion of concrete was investigated to determine the suitable mixed design for producing the lightweight concrete interlocking block. The laboratory tests were conducted to study the compressive strength and the diagonal tension (shear) strength of the block panel. The interlocking block was designed with a special shear key to enhance the shear strength of the block panel. In addition, the concrete block panels were strengthened with ferrocement technique and expanded

metal. The effects of mesh reinforcement on the compressive strength and the diagonal tension strength were investigated for various sizes of expanded metal.

2. Materials and Method

2.1. Water Treatment Sludge

The sludge was collected from Bang Khen water treatment plant and it was naturally sun-dried for two days with the residual water content of 7%. The dried sludge was crushed and ground under the Los Angle machine to reach the fine aggregate size according to ASTM C33/C33M-18 [22]. The appearance of the sun-dried material and the ground sludge are shown in Fig. 1a and Fig. 1b, respectively. The grain size distribution was determined by using sieve analysis, as shown in Fig. 2. Both of sludge and sand are consistent with boundary region. The fineness modulus and the specific gravity are 5.39 and 2.68 for the water treatment sludge, respectively.

a) Sun-dried sludge b) Ground sludge

Fig. 1. Water treatment sludge.

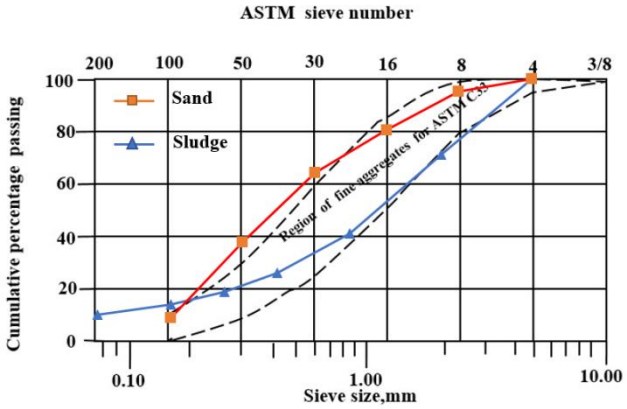

Fig. 2. Grain size distribution of sand and sludge.

2.2. Foaming Agent

The foaming agent was employed to produce cellular lightweight concrete by injecting a surfactant or a foaming agent into the cement paste. The microscopic air voids created in the concrete resulting to air-entrained concrete. The volume fraction of the foaming agent and the water was 1:30 which was appropriate for the foam generator capacity of 25 liters used in this study.

2.3. Expanded Metal

The expanded metal was the standard type overlapped diamond shape mesh pattern as shown in Fig. 3. Four types of expanded metal mesh were selected: No.22, No.23, XS-31, XS-32 conforming to JIS G3351 [23] which have the yield strength and the ultimate strength of 337 MPa and 400 MPa, repectively. The physical properties of the selected expanded metal are shown in Table 1. The specific surface of reinforcement (S_r) was defined as the total bonded area of expanded metal mesh divided by the volume of ferrocement.

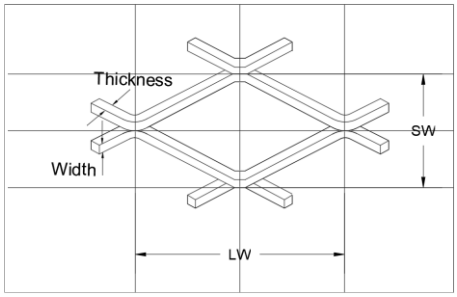

Fig. 3. Detail of expanded metal.

Table 1. Properties of expanded metal (JIS G3351-1987).

Type	SW (mm.)	LW (mm)	T (mm)	W (mm)	Weight (kg/m^2)	S_r (1/m)
No.22	8.6	20.0	0.6	0.6	0.69	0.0486
No.23	12.7	25.4	0.6	0.6	0.57	0.0338
XS-31	15.0	32.0	1.2	1.2	1.51	0.0565
XS-32	15.0	32.0	1.5	1.5	2.35	0.0707

2.4. Mixed Design of Concrete

The concrete composite was composed of portland cement type 1, sand, water treatment sludge, water, and foaming agent. The mixed proportion of these materials was determined for the appropriate admixture to meet the requirements of lightweight concrete block according to TIS 2601 [24]. The arrangement of laboratory test is presented in Table 2. The cement content was specified as a fixed value. The sand content was partially replaced by the sludge with the proportion of 0 – 60% of the fine aggregate by weight. The water content and the foam content were varied between 0.2-0.75 and 0.005-0.009 by weight of cement, respectively. The compressive strength, the density, and the absorption of the 5×5×5 cm mortar specimens were tested according to ASTM C109-02 [25] and ASTM C642-97 [26], respectively. In the first trial mix, it was to determine the optimum sludge and sand content. The obtained result from the mix no.1 was employed in the determination of water content (mix no.2). In the second trial mix, it was to determine the optimum water content. The result was applied in the determination of foam content (mix no. 3) leading to the final mix proportion.

DOI:10.4186/ej.2021.25.1.81

2.5. Concrete Block Prisms Test

Three sets of concrete block prisms were prepared as follows: a) concrete block prisms (CB-P) which are the standard concrete block typically used in the construction industry (Fig. 4a). This concrete block has the dimension and density which is similar to the interlocking block, therefore, it was chosen for comparison, b) the interlocking concrete block prisms prepared with thin bed adhesive mortar (IB1-P) commonly used in the construction of lightweight concrete block, and c) the interlocking concrete block prisms with thick bed cement mortar (IB2-P). The interlocking block was designed with 20 mm. corrugated shear keys at the upper and the lower surfaces (Fig. 4b). The 25 mm diameter hole at the center of block is provided for interlocking by cement grouting.

Details of the control specimens of the concrete block prisms (CB-P-CT), the interlocking block with thin bed adhesive mortar (IB1-P-CT), and interlocking block with thick bed cement mortar (IB2-P-CT) are presented in Fig. 5a, 5b, 5c, respectively. The bed mortar of CB-P-CT and IB2-P-CT was 25 mm thick cement mortar with cement and sand ratio of 1:2 by weight. For IB1-P-CT, the adhesive mortar with 3 mm thick was applied to bond each concrete block. The adhesive mortar was a dry bedding process which possessed high water retention without sprinkle water on the block. All specimens were plastered with 12 mm thick cement mortar for surface finishing.

Table 2. Mix proportions of lightweight composites.

Mix no.	Mixed Proportion (by weight)				
	Cement	Sand	Water	Foam	Sludge
1. Determination of sludge content	1.0	1.0	0.4	0.005	0
		0.9			0.1
		0.8			0.2
		0.7			0.3
		0.6			0.4
		0.5			0.5
		0.4			0.6
2. Determination of water content	1.0	0.7	0.20	0.005	0.3
			0.25		
			0.30		
			0.35		
			0.40		
			0.45		
			0.50		
			0.60		
			0.65		
			0.70		
			0.75		
3. Determination of foam content	1.0	0.7	0.60	0.005	0.3
				0.006	
				0.007	
				0.008	
				0.009	
4. Final mix design	1.0	0.7	0.60	0.006	0.3

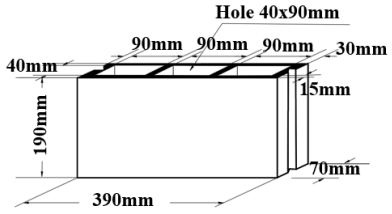

a) Concrete block

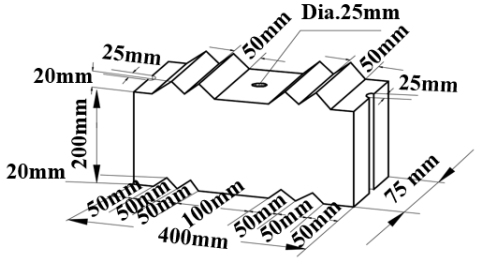

b) Interlocking Concrete Block

Fig. 4. Details of concrete blocks.

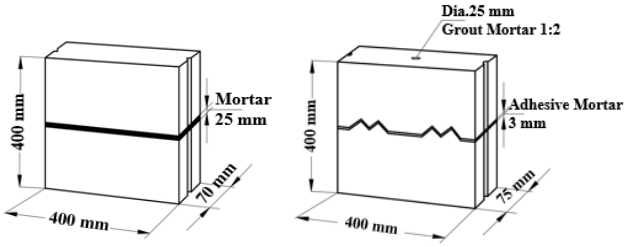

a) CB-P-CT b) IB1-P-CT (thin bed adhesive mortar)

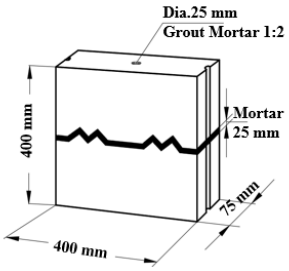

c) IB2-P-CT (thick bed cement mortar)

Fig. 5. Details of concrete block prisms.

For the strengthened specimens, the three sets of concrete blocks were strengthened by using the expanded metal mesh No.22, No.23, XS-31, XS-32. The chicken wire meshes: the 0.71 mm diameter square mesh (SM) and the 0.50 mm diameter hexagonal mesh (HM) were also applied for comparison. The chicken meshes are made of galvanized iron with a tensile strength of 260 Mpa. These were attached at both sides of the specimens connected with 6 mm diameter screw. All specimens were finished by plastering with 12 mm thick cement mortar. The strengthened prisms of the concrete block (CB-P-S), the interlocking block with thin bed adhesive mortar (IB1-P-S), and interlocking block with thick bed cement mortar (IB2-P-S) are presented in Fig. 6a, 6b, 6c, respectively. The designated symbol S stands for the strengthened specimen, and it was later replaced by 22, 23, 31, 32, 33, SM, HM corresponding to the

expanded metal and the wire mesh types. For each set of concrete blocks, the total 21 specimens were prepared for the 7 prism types with 3 specimens for each type. The concrete prisms were tested for 28 days strength according to ASTM C1314-07 [27] (Fig. 6d). In this study, the correction factor of 1.15 was considered for the corresponding height and thickness ratio as recommended by the ASTM C1314-07 [27].

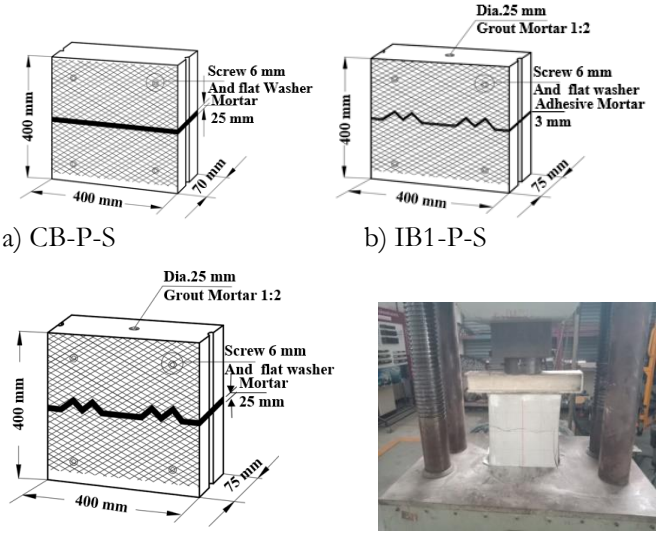

a) CB-P-S b) IB1-P-S

c) IB2-P-S d) Prism test

Fig. 6. Details of strengthened concrete block prisms.

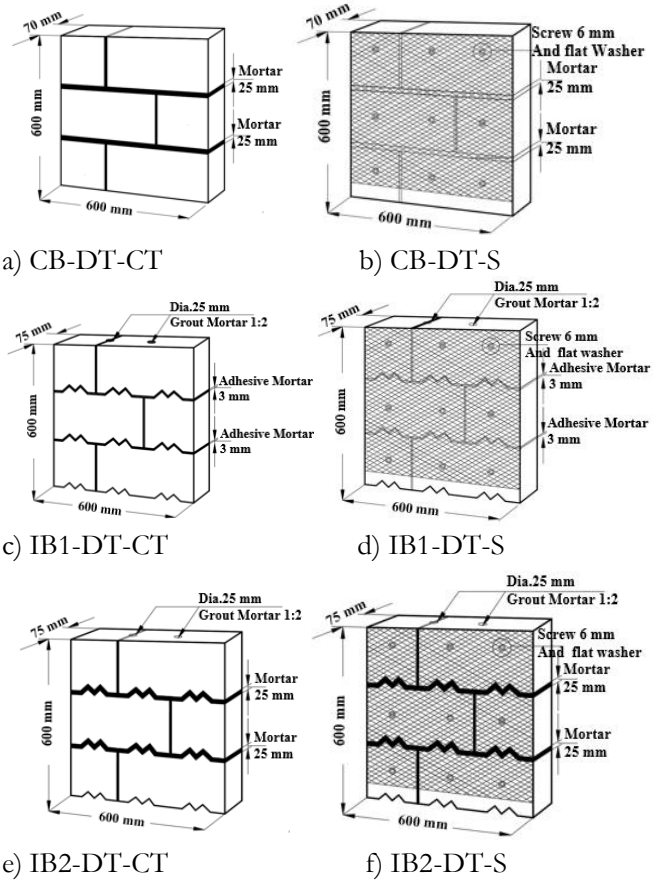

a) CB-DT-CT b) CB-DT-S

c) IB1-DT-CT d) IB1-DT-S

e) IB2-DT-CT f) IB2-DT-S

Fig. 7. Concrete blocks for Diagonal Tension Test.

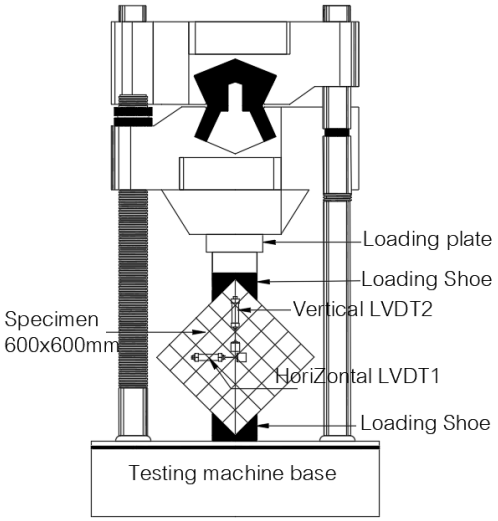

Fig. 8. Diagonal Tension Test.

2.6. Diagonal Tension Test

Three sets of concrete block panels were prepared for diagonal tension testing as follows: a) concrete block panels (CB-DT), b) the interlocking concrete block panels with thin bed adhesive mortar (IB1-DT), and c) the interlocking concrete block panels with thick bed cement mortar (IB2-DT). The block panels were prepared for 600×600 mm square. The holes were filled with the cement mortar with the cement and sand ratio of 1:2.

The strengthened panels were prepared similar to those of the prism test. The control (CT) and the strengthened panels (S) for CB, IB1, IB2 are presented in Fig. 7a-7b, 7c-7d, 7e-7f, respectively. Three sets of block panels were strengthened by using the expanded metal mesh No. 22, No.23, XS-31, XS-32, and the wire mesh SM, HM. For each set of block panels, the total 21 specimens were prepared for the 7 panel types with 3 specimens for each type. The block panels were tested for 28 days diagonal tension strength according to ASTM E519-02 [28] (Fig. 8). The LVDT instruments were installed in the vertical and horizontal directions to measure the displacement of the specimen under loading.

3. Experimental Results

3.1. Concrete Mixed Proportion

The first trial mix design was to determine the suitable sludge content for the variation of sludge and fine aggregate ratio. The results of compressive strength including density and the water absorption versus the sludge content for 7 days curing are presented in Fig. 9a, 9b, respectively.

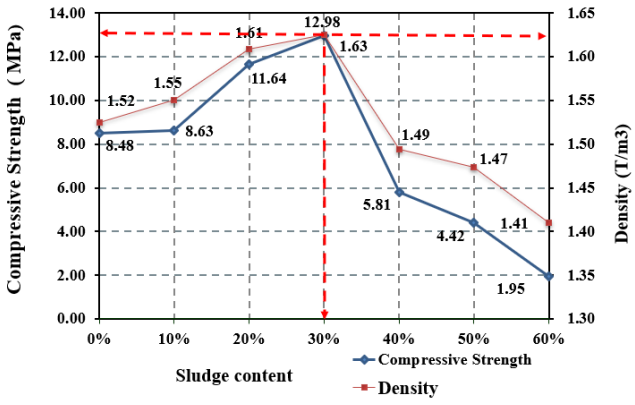

a) Strength and density

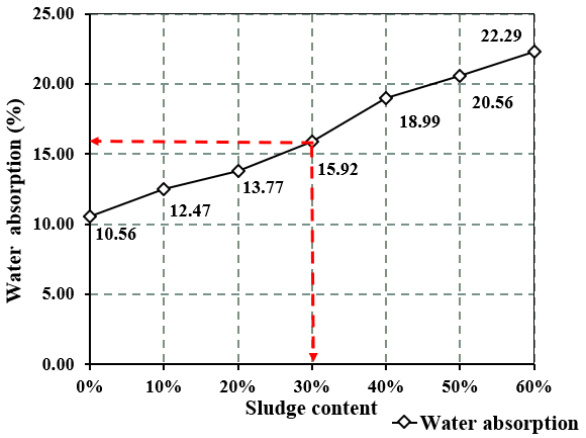

b) Water absorption

Fig. 9. Compressive strength, density and the water absorption versus the sludge content.

It was found that the compressive strength and density were increased with the addition of sludge content up to 30%. The beneficial effect of additional sludge content on the compressive strength was due to the balancing of water content of the cement hydration owing to the water absorption of sludge. The water treatment sludge possess high water absorption characteristic which could absorb the excessive water to reach the optimum hydration of cement paste. However, the over demand of sludge content caused large amount of water absorption resulting to the lack of water for cement hydration, and hence adverse effect on the compressive strength. The effect of additional sludge content on the density was conforming to the balancing of water content of the cement hydration. The absorbed water at the less sludge content caused more cement hydration, and it contributed to more dense cement paste up to the optimum hydration. The oversupply sludge content led to the porous cement paste, and hence less dense cement paste. Eventually, the optimum sludge content of 30% provided the compressive strength of 12.98 Mpa, the density of 1.63 Ton/m^3 and the water absorption of 15.92% conforming to the lightweight concrete class C16 according to TIS 2601-13 [24].

The second mix design was to determine the suitable water content by applying the optimum sludge content of 30% in the mix proportion. The results of compressive strength including density and the water absorption versus the water content obtained from 12 sets of mortar specimens for 7 days curing are presented in Fig. 10a, 10b, respectively.

The compressive strength was steadily increased with the addition of water content due to the presence of water treatment sludge that required additional water for the hydrated reaction. The cement hydration continued with the increase of w/c ratio. Meanwhile, the cement paste gained more strength and density up to the optimum water content. The oversupply water made the more porous cement paste resulting to the adverse effect of compressive strength and the less density. The optimum water content was required up to 60% of cement by weight that provided the compressive strength of 15.22 MPa and the density of 1.65 T/m^3, and the water absorption of 19.55%. The obtained results are conforming to the lightweight concrete class C16 according to TIS 2601-13 [24].

The third mix design was to determine the suitable foaming agent content by applying the optimum sludge content of 30% and water content of 60% in the mix proportion. The results of compressive strength including density and the water absorption versus the foam content obtained from 5 sets of mortar specimens for 7 days curing are presented in Fig. 11a, 11b, respectively.

The compressive strength and density were continuously decreased with the addition of foaming agent content due to the increase of microscopic air voids causing more air-entrained concrete.

The foam content of 0.6% was selected as the optimum consistency of mixture that provided the compressive strength of 15.40 MPa and the density of 1.65 T/m^3, and the water absorption of 17.92%. The obtained results are conforming to the lightweight concrete class C16 according to TIS 2601-13 [24].

Therefore, the appropriate mix proportion was considered as the final mix presented in Table 2. The final mix proportion was verified by testing the 150×150×150 mm cement mortar for compressive strength, density and water absorption. The interlocking concrete block with the final mix proportion was also tested for the compressive strength according to TIS 109-74 [29]. The test results of 28 days curing are presented in Table 3. The test results of cement mortar are conforming to the lightweight concrete class C16 according to TIS 2601-13 [24]. In addition, the compressive strength of the interlocking concrete block is higher than the specified strength of 2.0 Mpa for non-load-bearing concrete block according to TIS 58-87 [30] and it is also higher than the compressive strength of ordinary concrete block (2.34 MPa). While the density (1,700 kg/m^3) of the ordinary concrete block is comparable to the interlocking concrete block.

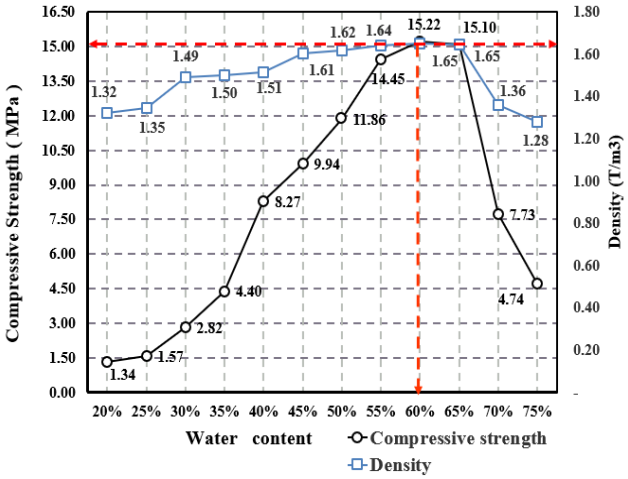

a) Strength and density

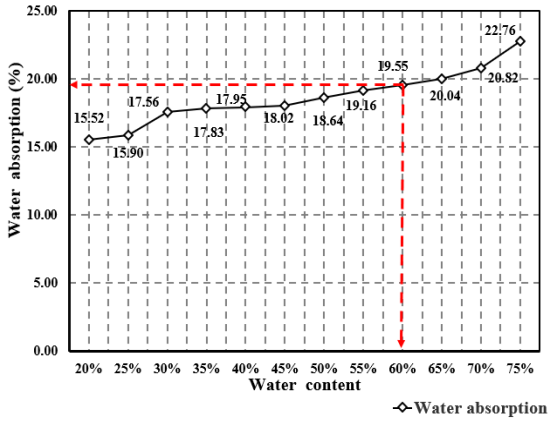

b) Water absorption

Fig. 10. Compressive strength, density and the water absorption versus the water content.

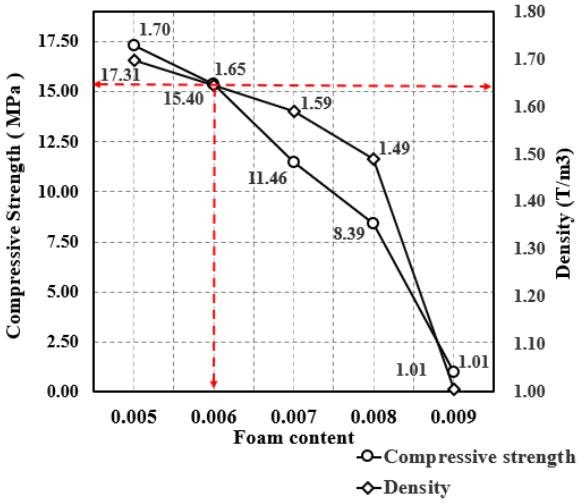

a) Strength and density

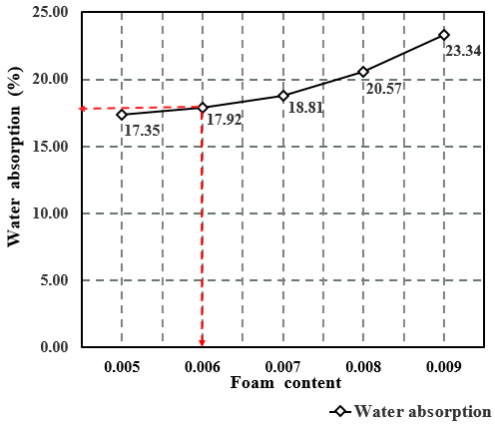

b) Water absorption

Fig. 11. Compressive strength, density and the water absorption versus the foam content.

Table 3. Properties of cement mortar and interlocking block.

Specimens	Strength (Mpa)	Density (kg/m^3)	Absorption (%)
Cement mortar	16.4	1640	16.87
Interlocking block	5.0	1600	16.82

3.2. Results of Concrete Block Prisms

The failure mechanism of the three sets of concrete block prisms: concrete block (CB), interlocking block (IB1), and interlocking block (IB2) are presented in Fig.12a-12g, Fig.13a-13g, and Fig.14a-14g, respectively. The failure modes indicated by the arrows with abbreviations as shown in these figures are summarized in Table 4. The concrete block (CB) prisms were failed under bilateral tension causing the vertical spalling cracks at both surfaces of the specimens which are face shell separation mode for all specimens. The failure mechanism was due to the internal stress in concrete block under prism test illustrated in Fig. 15a. When the prism was subjected to the vertical compressive stress, the concrete block was expanded in the lateral direction more than the bed mortar. Since the compressive strength of concrete block was lower than that of the bed mortar, and hence the lower elastic modulus, this created the bilateral tension in the concrete block. Meanwhile, the bed mortar was confined with the concrete block, resulting to the tri-axial compression within bed mortar. The stress equilibrium in the lateral direction created the bilateral tension in the concrete block causing the spalling crack at both sides of prism. For the strengthened specimens with the expanded metal mesh (CB-P-22, CB-P-23, CB-P-31, CB-P-32) including the specimens with wire mesh (CB-P-SM, CB-P-HM), the effect of reinforcement enhanced the tensile strength of concrete prisms resulting to the increase of compressive strength of the prisms. It can be observed that the plastered cement mortar of the prism strengthened with hexagonal wire mesh (CB-P-HM) was slipped off due to

DOI:10.4186/ej.2021.25.1.81

insufficient bond strength between the wire mesh and the concrete panel. The debonding was caused by the insufficient embedded length of the screw penetrated in the hollow concrete block.

For the mechanism of interlocking block, the internal stress under prism test is presented in Fig. 15b. The bilateral stress created shear stress along the interface between the bed mortar and the shear key. The longitudinal shear strength (x-axis) is greater than that of the transverse direction (y-axis) due to the corrugated interlocking shear key. The control specimen of the interlocking block with thin bed adhesive mortar (IB1-P-CT) was failed under lateral buckling in the weaker plane resulting in tension break failure mode observed by the horizontal crack of bed mortar between each interlocking block. This indicated that adhesive mortar typically used in the construction of lightweight concrete block provided insufficient bond strength between interlocking block. However, the strengthened specimens with expanded metal mesh (IB1-P-22, IB1-P-23, IB1-P-31, IB1-P-32) including the specimens with wire mesh (IB1-P-SM, IB1-P-HM) protected against lateral buckling in the weaker plane without tension break failure, the lateral strength was enhanced, therefore, the failure mechanism of all strengthened specimens was changed to face shell separation mode.

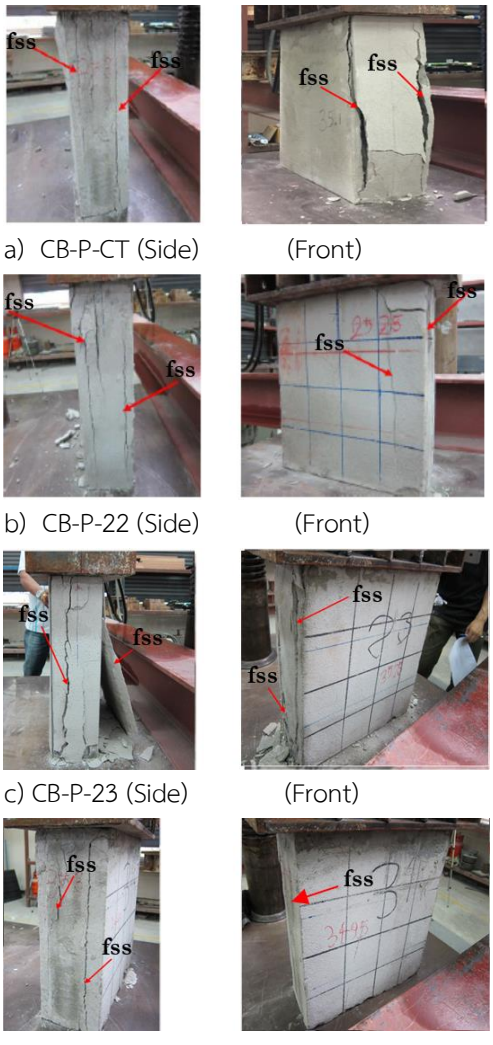

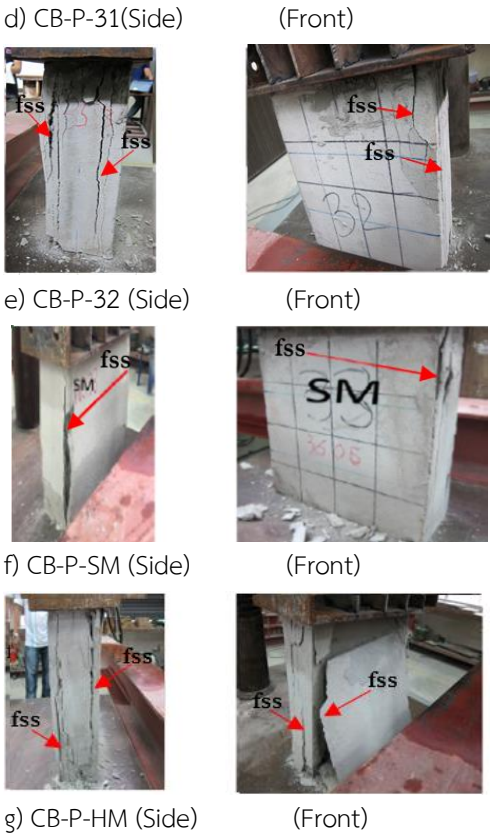

Fig. 12. Failure of Concrete Block, CB (Prism test).

The control specimen of the interlocking block with thick bed cement mortar (IB2-P-CT) was failed under shear break failure mode observed by the diagonal crack of the end section of the interlocking block. The horizontal crack passed through the interlocking block without any crack at the bed mortar. This indicated that the thick bed cement mortar was superior to the thin bed adhesive mortar typically used in the construction of lightweight concrete. In contrast, the strengthened specimens with expanded metal mesh (IB2-P-22, IB2-P-23, IB2-P-31, IB2-P-32) including the specimens with wire mesh (IB2-P-SM, IB2-P-HM) protected against the shear break failure, and the failure mechanism of all strengthened specimens was face shell separation mode.

The stress-strain relationship of the three sets of concrete block prisms are presented in Fig. 16. It is obvious that the compressive strength values of all types of the strengthened specimens are greater than that of the control specimen. Among the strengthened specimens, the expanded metal meshes provided the greater compressive strength than those of the wire meshes (SM and HM) due to the superior bonding between the mesh and the block prisms. The expanded metal meshes are divided into 2 groups: a) small meshes, i.e, No.22 and No.23, b) large meshes, i.e, XS31, XS32.

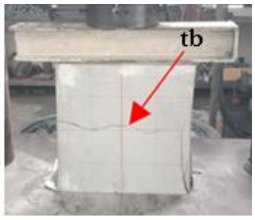

a) IB1-P-CT

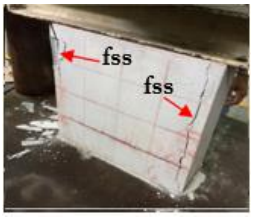

b) IB1-P-22

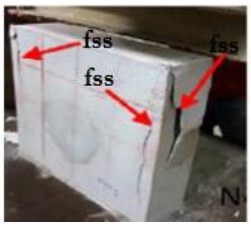

c) IB1-P-23

d) IB1-P-31

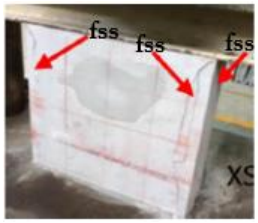

e) IB1-P-32

f) IB1-P-SM

g) IB1-P-HM

Fig. 13. Failure of interlocking block IB1 (Prism test).

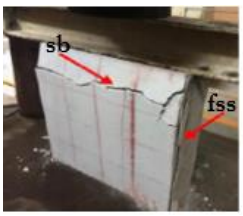

a) IB2-P-CT

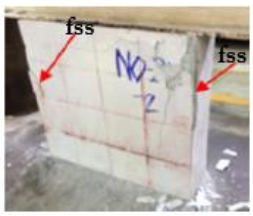

b) IB2-P-22

c) IB2-P-23

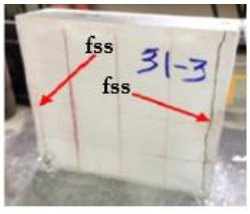

d) IB2-P-31

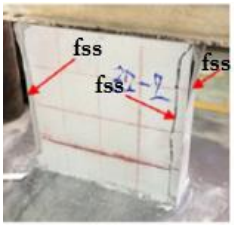

e) IB2-P-32

f) IB2-P-SM

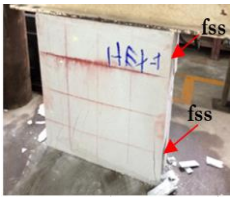

g) IB2-P-HM

Fig. 14. Failure of interlocking block IB2 (Prism test).

Table 4. Failure modes of prism tests.

Specimens	Failure modes
CB-P-CT	Face shell separation (fss)
IB1-P-CT	Tension break (ts)
IB2-P-CT	Shear break (sb)
CB-P-22, IB1-P-22, IB2-P-22	Face shell separation (fss)
CB-P-23, IB1-P-23, IB2-P23	Face shell separation (fss)
CB-P-31, IB1-P-31, IB2-P-31	Face shell separation (fss)
CB-P-32, IB1-P-32, IB2-P-32	Face shell separation (fss)
CB-P-SM, IB1-P-SM, IB2-P-SM	Face shell separation (fss)
CB-P-HM, IB1-P-HM, IB2-P-HM	Face shell separation (fss)

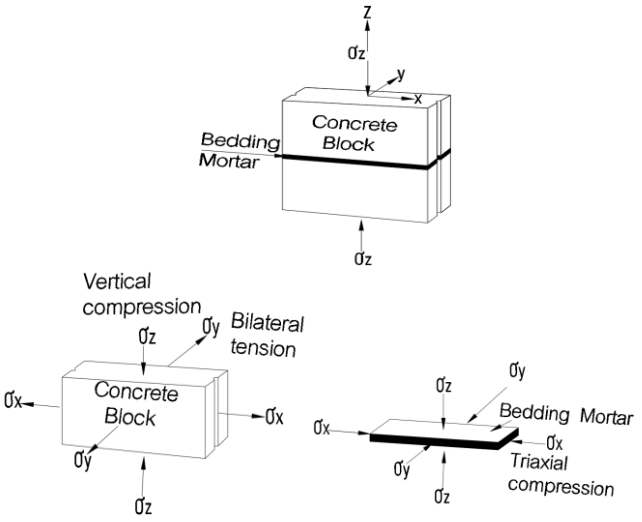

a) Concrete block

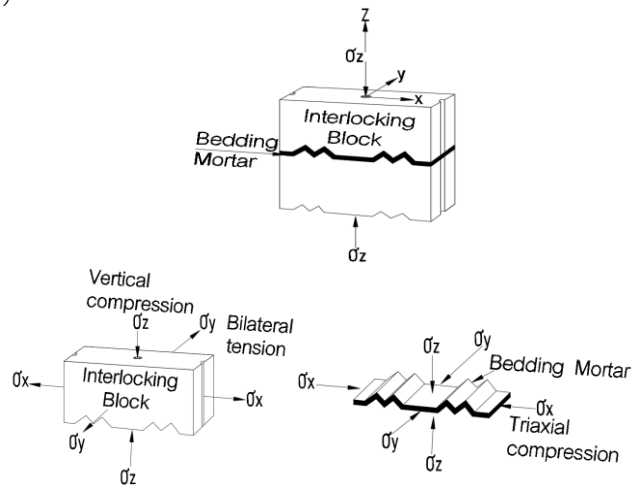

b) Interlocking block

Fig. 15. Stress in concrete block under prism test.

For the small meshes, the expanded metal No. 22 provided higher strength than that of No. 23 due to the greater value of the specific surface of reinforcement of No. 22 (S_r = 0.0486 m^{-1}) when compared with that of No.23 (S_r = 0.0338 m^{-1}), as presented in Table 1. The high value of S_r enhanced the bond strength between the mesh and the block panel resulting to the high compressive strength of prism. For the case of large meshes, the compressive strength of XS31, XS32 specimens are lower than the small meshes. Although the S_r values of large meshes are greater than the small mesh, the large meshes possess thicker and larger mesh sizes, and hence the large meshed are stiffer than the small meshes. The lath plane did not uniformly attach with the block surface, as a result, debonding occurred under loading. The large meshes could not achieve their load carrying capacity corresponding to their mesh sizes. Additional investigation is required for further study to improve the efficiency of expanded metal mesh such as the strengthening with the addition of tightened bolts.

The comparison among the three sets of the prism tests revealed that the compressive strength of thin bed adhesive mortar interlocking block prisms (IB1-P) are higher than the concrete block (CB-P) for both control specimen and strengthened specimens. The effect of shear key for interlocking block enhanced the bond strength between each concrete block when compared to the conventional block. In addition, the thick bed cement mortar interlocking block prisms (IB2-P) is superior to the thin bed adhesive mortar interlocking block prisms (IB1-P). The compressive strength of IB2-P was significantly enhanced due to the high adhesive strength of cement mortar with thick bed improved the bond strength transmitted by the shear key between each interlocking block.

The strength and ductility capacity of concrete block prisms CB, IB1, IB2 are considered from the stress-stain relationships. The strength and strain corresponding to the yiled and the maximum points were determined based on the method presented by P. Panyakapo [31]. The results of CB-P, IB1-P, IB2-P are shown in Table 5, 6, 7, respectively. For the concrete block, the strengthened specimens with expanded metal (CB-P-22, CB-P-23, CB-P-31, CB-P-32) provided the load capacity 1.56, 1.47, 1.36, 1.33 times that of the control specimen, respectively. Similarly, the ductility capacity was 4.90, 3.91, 2.51, 2.47 times that of the control specimen.

For the thin bed adhesive mortar interlocking block prisms (IB1-P), the strengthened specimens with expanded metal (IB1-P-22, IB1-P-23, IB1-P-31, IB1-P-32) provided the load capacity 1.77, 1.54, 1.36, 1.28 times that of the control specimen, respectively. Similarly, the ductility capacity was 4.21, 3.29, 3.14, 2.97 times that of the control specimen.

For the thick bed cement mortar interlocking block prisms (IB2-P), the strengthened specimens with expanded metal (IB2-P-22, IB2-P-23, IB2-P-31, IB2-P-32) enhanced the load capacity up to 2.00, 1.73, 1.43, 1.42 times that of the control specimen, respectively. Similarly, the ductility capacity was significantly increased by 6.48, 5.71, 4.55, 3.91 times that of the control specimen. It was noticed that the strength and ductility of specimens with expanded metal are greater than that of the wire meshed (SM, HM) for all types of concrete blocks. The effects of mesh type with overlapped diamond shape of the expanded metal contributed the strength and ductility that is superior to the conventional wire mesh.

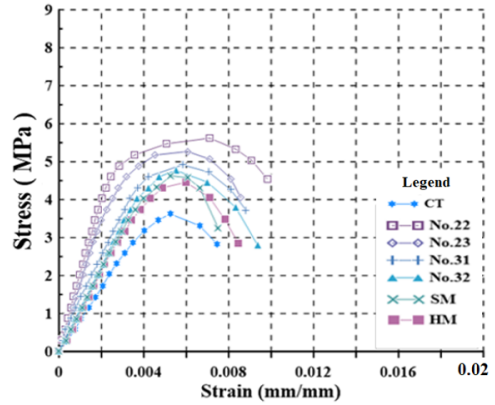

a) Concrete block (CB-P)

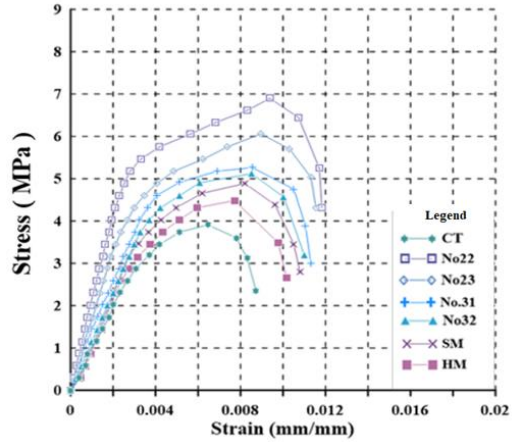

b) Interlocking block (IB1-P)

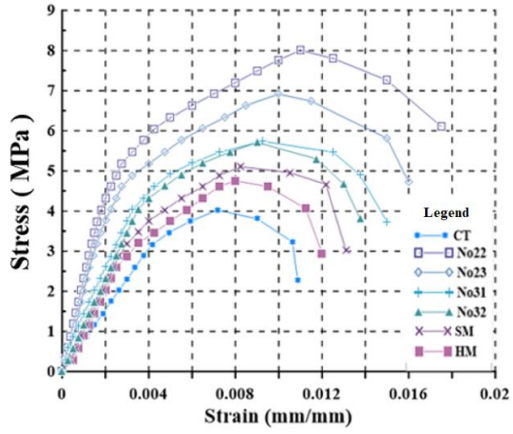

c) Interlocking block (IB2-P)

Fig. 16. Stress-strain relationship of concrete block prisms.

The comparison among the control specimens of CB-P-CT, IB1-P-CT, IB2-P-CT revealed that the effect of shear key for the interlocking block enhanced the strength by 8% and 11% for IB1-P-CT, IB2-P-CT, respectively. But, the effect of shear key caused an increase of the ductility capacity by 19% and 32% for IB1-P-CT, IB2-P-CT, respectively. Therefore, the contribution of shear key for the interlocking block significantly affected to the ductility capacity rather than the strength. In additional, the prism test results indicated that the strength and the ductility capacity of the strengthened specimens were significantly improved due to the effects of ferrocement with expanded mental as well as the wire mesh. It was observed that among the strengthened specimens, the strength of IB2-P-22, IB2-P-23, IB2-P-31, IB2-P-32 were greater than the IB1-P-22, IB1-P-23, IB1-P-31, IB1-P-32 by 13%, 12%, 5%, 11%, respectively. Similarly, the ductility capacity was increased by 54%, 74%, 45%, 32%, respectively. Therefore, the thick bed cement mortar contributed more strength and ductility capacity than the thin bed adhesive mortar.

Table 5. Strength and ductility capacity of concrete block prism (CB-P).

Specimen	Yield Strength (MPa)	Yield Strain (mm/mm)	Max. Strength (MPa)	Max. Strain (mm/mm)	Load Capacity	Ductility
CB-P-CT	3.0	0.0038	3.6	0.0075	1.0	1.97
CB-P-22	4.0	0.0020	5.6	0.0098	1.56	4.90
CB-P-23	4.3	0.0022	5.3	0.0086	1.47	3.91
CB-P-31	4.3	0.0035	4.9	0.0088	1.36	2.51
CB-P-32	4.0	0.0038	4.8	0.0094	1.33	2.47
CB-P-SM	3.8	0.0032	4.6	0.0075	1.28	2.3
CB-P-HM	3.8	0.0038	4.5	0.0084	1.25	2.21

Table 6. Strength and ductility capacity of interlocking block prism (IB1-P).

Specimen	Yield Strength (MPa)	Yield Strain (mm/mm)	Max. Strength (MPa)	Max. Strain (mm/mm)	Load Capacity	Ductility
IB1-P-CT	3.2	0.0037	3.9	0.0087	1.0	2.35
IB1-P-22	5.0	0.0028	6.9	0.0118	1.77	4.21
IB1-P-23	4.3	0.0035	6.0	0.0115	1.54	3.29
IB1-P-31	4.0	0.0036	5.3	0.0113	1.36	3.14
IB1-P-32	3.8	0.0037	5.0	0.0110	1.28	2.97
IB1-P-SM	3.5	0.0037	4.9	0.0108	1.26	2.92
IB1-P-HM	3.2	0.0036	4.5	0.0102	1.15	2.83

Table 7. Strength and ductility capacity of interlocking block prism (IB2-P).

Specimen	Yield Strength (MPa)	Yield Strain (mm/mm)	Max. Strength (MPa)	Max. Strain (mm/mm)	Load Capacity	Ductility
IB2-P-CT	3.2	0.0042	4.0	0.0109	1.0	2.60
IB2-P-22	5.2	0.0027	8.0	0.0175	2.00	6.48
IB2-P-23	4.6	0.0028	6.9	0.0160	1.73	5.71
IB2-P-31	4.0	0.0033	5.7	0.0150	1.43	4.55
IB2-P-32	4.0	0.0035	5.7	0.0137	1.42	3.91
IB2-P-SM	3.4	0.0036	5.0	0.0131	1.25	3.64
IB2-P-HM	3.3	0.0038	4.8	0.0120	1.19	3.16

3.3. Results of Diagonal Tension

The failure mechanism of the three sets of concrete block panels: concrete block (CB), interlocking block (IB1), and interlocking block (IB2) are presented in Fig. 17a-17g, Fig. 18a-18g, and Fig. 19a-19 g, respectively. The failure modes indicated by the arrows with abbreviations as shown in these figures are summarized in Table 8. It was observed that the concrete block panels (CB-DT) were failed in shear due to diagonal tension indicated by the diagonal crack in the vertical direction. The diagonal tension was caused by the internal expansive stress exerted in the horizontal direction orthogonal to the applied vertical stress. It was noticed that all of the strengthened block panels also failed due to diagonal tension. In addition, debonding of the ferrocement was observed with the face shell separation for the specimen CB-DT-23 because the hollow core of concrete block caused insufficient bond strength between the screw and the concrete block. The hollow core of concrete block also affected on the strengthened specimen with expanded metal xs32 (CB-DT-32), which was failed by the corner compression mode due to the stress concentration at the loading shoe.

For the interlocking block panels with thin bed adhesive mortar (IB1), all of the specimens were failed in shear due to diagonal tension without any face shell separation failure. Similar results were also found for the case of the interlocking block panels with thick bed cement mortar (IB2).

DOI:10.4186/ej.2021.25.1.81

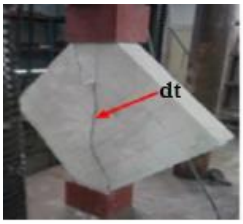

a) CB-DT-CT

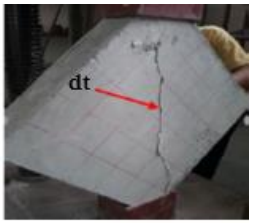

b) CB-DT-22

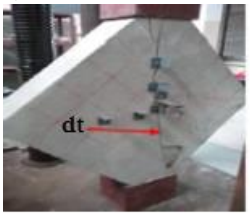

c) CB-DT-23 (Front)

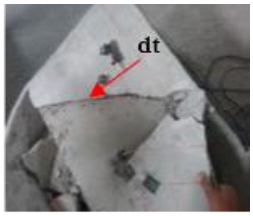

(Back)

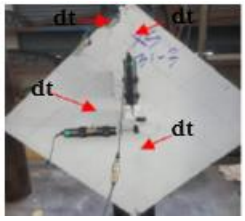

d) CB-DT-31 (Front)

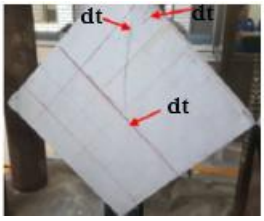

(Back)

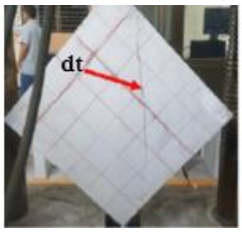

e) CB-DT-32 (Front)

(Back)

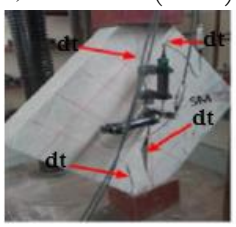

f) CB-DT-SM (Front)

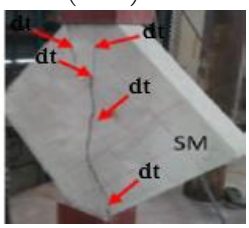

(Back)

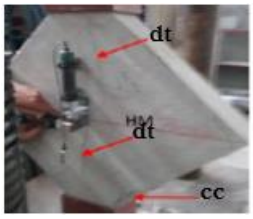

g) CB-DT-HM(Front)

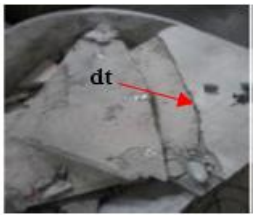

(Back)

Fig. 17. Failure of Diagonal Tension test (CB).

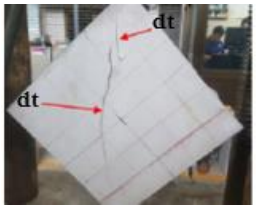

a) IB1-DT-CT

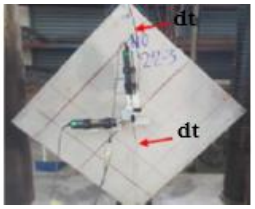

b) IB1-DT-22

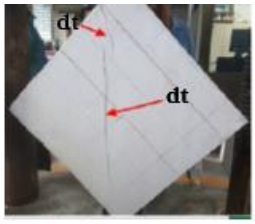

c) IB1-DT-23

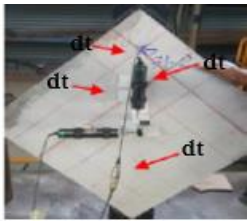

d)IB1-DT-31

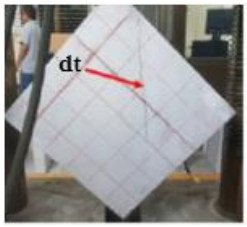

e) IB1-DT-32

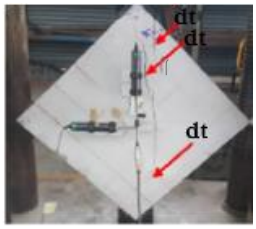

f) IB1-DT-SM

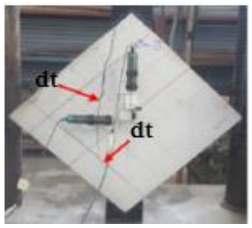

g) IB1-DT-HM

Fig. 18. Failure of Diagonal Tension test (IB1).

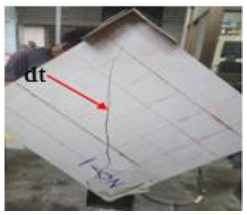

a) IB2-DT-CT

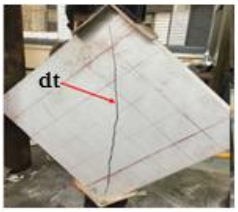

b) IB2-DT-22

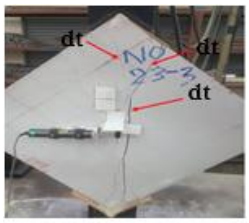

c) IB2-DT-23

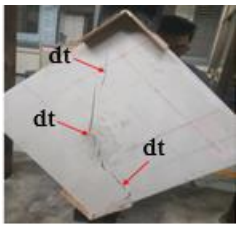

d) IB2-DT-31

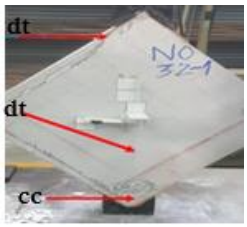

e) IB2-DT-32

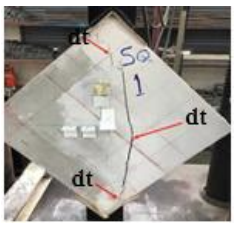

f) IB2-DT-SM

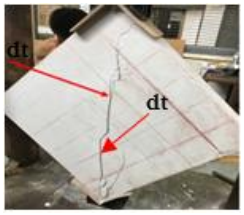

g) IB2-DT-HM

Fig. 19. Failure of Diagonal Tension test (IB2).

Table 8. Failure modes of diagonal tests.

Specimens	Failure modes
CB-DT-CT, IB1-DT-CT, IB2-DT-CT	Diagonal tension (dt)
CB-DT-22, IB1-DT-22, IB2-DT-22	Diagonal tension (dt)
CB-DT-23, IB1-DT-23, IB2-DT-23	Diagonal tension (dt)
CB-DT-31, IB1-DT-31, IB2-DT-31	Diagonal tension (dt)
CB-DT-32, IB2-DT-32, CB-DT-HM	Diagonal tension (dt) and Corner compression (cc)
IB1-DT-32	Diagonal tension (dt)
CB-DT-SM, IB1-DT-SM, IB2-DT-SM	Diagonal tension (dt)
IB1-DT-HM, IB2-DT-HM	Diagonal tension (dt)

The stress-strain relationships of the three sets of concrete block prisms are presented in Fig. 20. Among the control specimens CB-DT-CT, IB1-DT-CT, IB2-DT-CT (Fig. 20a, Fig. 20b, Fig. 20c), the shear strength of the interlocking block IB1-DT-CT and IB2-DT-CT were enhanced by 21%, 34%, respectively compared to the conventional concrete block. This indicated that the use of shear key for interlocking block could improve the shear strength of the concrete block.

The stress-strain relationships of the three sets of concrete block were determined for the yield shear strength (S_{sy}), ultimate shear strength (S_{su}), yield shear strain (γ_y), modulus of rigidity (G), modulus of elasticity (E), as shown in Tables 9-11.

It is evidenced that the ultimate shear strength (S_{su}) and the modulus of rigidity (G) of all types of the strengthened specimens are greater than that of the control specimen. For the concrete block (CB, Table 9) the shear strength (S_s) of the strengthened concrete blocks was increased by 72%, 49%, 40%, 34%, 23%, 21%, for CB-DT-22, CB-DT-23, CB-DT-31, CB-DT-32, CB-DT-SM, CB-DT-HM, respectively. Similarly, the modulus of rigidity (G) of the strengthened concrete blocks was increased by 99%, 68%, 58%, 37%, 24%, 3%, respectively.

For the interlocking block (IB1, Table 10) the shear strength (S_s) of the strengthened interlocking blocks was increased by 63%, 47%, 42%, 39%, 33%, 9%, for IB1-DT-22, IB1-DT-23, IB1-DT-31, IB1-DT-32, IB1-DT-SM, IB1-DT-HM, compared to the control specimen, respectively. Similarly, the modulus of rigidity (G) of the strengthened interlocking blocks was increased by 95%, 81%, 71%, 32%, 30%, 2%, respectively.

For the interlocking block (IB2, Table 11) the shear strength (S_s) of the strengthened interlocking blocks was increased by 79%, 63%, 55%, 49%, 44%, 11%, for IB2-DT-22, IB2-DT-23, IB2-DT-31, IB2-DT-32, IB2-DT-SM, IB2-DT-HM, compared to the control specimen, respectively. Similarly, the modulus of rigidity (G) of the strengthened interlocking blocks was increased by 79%, 70%, 68%, 43%, 36%, 33%, respectively.

The comparison between the strengthened specimens IB1-DT and IB2-DT (Fig. 20b vs Fig. 20c and Table 10 vs Table 11) revealed that the strengthened interlocking blocks (IB2-DT) was superior to that of IB1-DT. The shear strength (S_s) was enhanced by 21.5%, 22.6%, 21.0%, 19.0%, 19.7%, 12.9%, for IB2-DT-22, IB2-DT-23, IB2-DT-31, IB2-DT-32, IB2-DT-SM, IB2-DT-HM, compared to that of IB1-DT, respectively. The modulus of rigidity (G) and the modulus of elasticity (E) were improved as well. This indicated that the shear key with thick bed cement mortar is more effective than the thin bed adhesive mortar typically used in the construction of lightweight concrete.

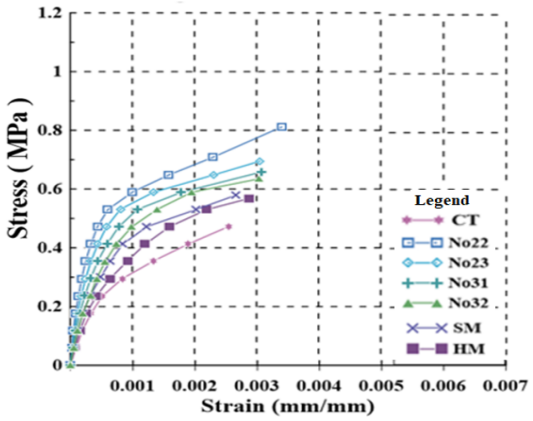

a) Concrete block (CB-DT)

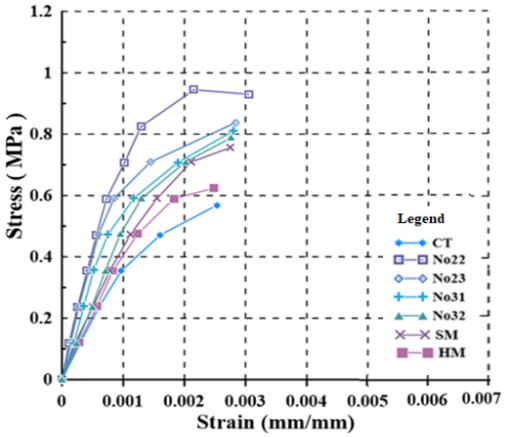

b) Interlocking block (IB1-DT)

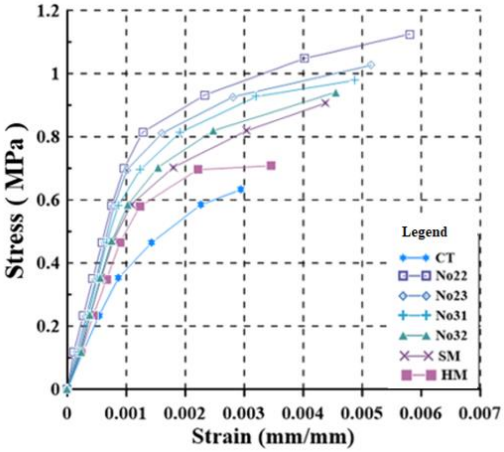

c) Interlocking block (IB2-DT)

Fig. 20. Shear stress and shear strain of the diagonal tension test.

Table 9. Shear strength and shear strain of concrete block (CB-DT).

Specimen	S_{sy} (MPa)	S_{su} (MPa)	γ_y (mm/mm)	G (MPa)	E (MPa)
CB-DT-CT	0.29	0.47	0.00084	345.24	863.10
CB-DT-22	0.53	0.81	0.00077	688.31	1720.78
CB-DT-23	0.47	0.70	0.00081	580.25	1450.62
CB-DT-31	0.41	0.66	0.00075	546.67	1366.67
CB-DT-32	0.35	0.63	0.00074	472.97	1182.43
CB-DT-SM	0.32	0.58	0.00075	426.67	1066.67
CB-DT-HM	0.30	0.57	0.00084	357.14	892.86

Table 10. Shear strength and shear strain of interlocking block (IB1-DT).

Specimen	S_{sy} (MPa)	S_{su} (MPa)	γ_y (mm/mm)	G (MPa)	E (MPa)
IB1-DT-CT	0.35	0.57	0.00096	368.75	921.88
IB1-DT-22	0.59	0.93	0.00082	719.51	1798.78
IB1-DT-23	0.58	0.84	0.00087	666.67	1666.67
IB1-DT-31	0.47	0.81	0.00075	632.00	1580.00
IB1-DT-32	0.46	0.79	0.00095	487.37	1218.42
IB1-DT-SM	0.37	0.76	0.00078	479.49	1198.72
IB1-DT-HM	0.36	0.62	0.00097	375.26	938.14

Table 11. Shear strength and shear strain of interlocking block (IB2-DT).

Specimen	S_{sy} (MPa)	S_{su} (MPa)	γ_y (mm/mm)	G (MPa)	E (MPa)
IB2-DT-CT	0.35	0.63	0.00086	406.98	1017.44
IB2-DT-22	0.72	1.13	0.00099	727.27	1818.18
IB2-DT-23	0.69	1.03	0.00100	690.00	1725.00
IB2-DT-31	0.59	0.98	0.00086	686.05	1715.12
IB2-DT-32	0.58	0.94	0.00100	580.00	1450.00
IB2-DT-SM	0.57	0.91	0.00103	553.40	1383.50
IB2-DT-HM	0.47	0.70	0.00087	540.23	1350.57

3.4. Analytical Results

The relationships between the maximum compressive strength, f'_m and the specific surface of reinforcement, S_r obtained from the prism test are presented in Eq. (1)-(3) and Fig. 21 for CB, IB1, IB2, respectively.

For CB: $f'_m = 3.63 + 80.98S_r - 932.14S_r^2$ (1)

For IB1: $f'_m = 3.91 + 117.77S_r - 1450.2S_r^2$ (2)

For IB2: $f'_m = 4.03 + 154.6S_r - 1896.1S_r^2$ (3)

The results of the shear strength (S_{su}) are also presented in Eq. (4)-(6) and Fig. 22 for CB, IB1, IB2, respectively.

For CB: $S_{su} = 0.47 + 12.69S_r - 147.7S_r^2$ (4)

For IB1: $S_{su} = 0.57 + 13.77S_r - 152.07S_r^2$ (5)

For IB2: $S_{su} = 0.63 + 19.49S_r - 216.39S_r^2$ (6)

The expressions between f'_m, S_{su} and S_r were evaluated by nonlinear regression analysis. These expressions are useful to predict the compressive strength and the shear strength of the strengthened specimens with various specific surface of reinforcement. It should be remarked that the strength degradation after the post-peak strength was due to the effects of the larger size mesh of expanded metal that explained in the previous section.

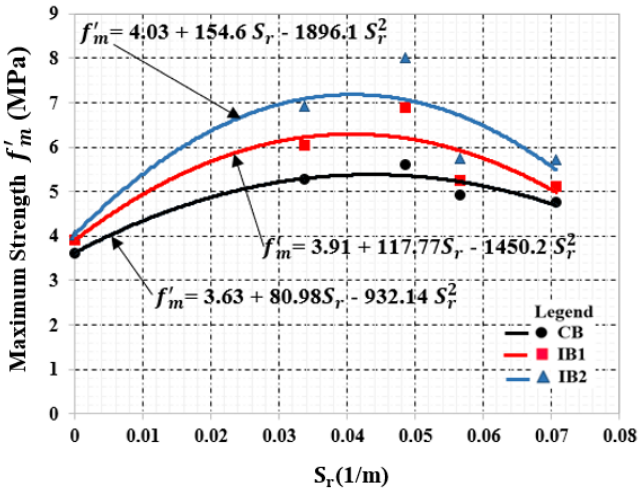

Fig. 21. Maximum compressive strength and specific surface of reinforcement for prism test.

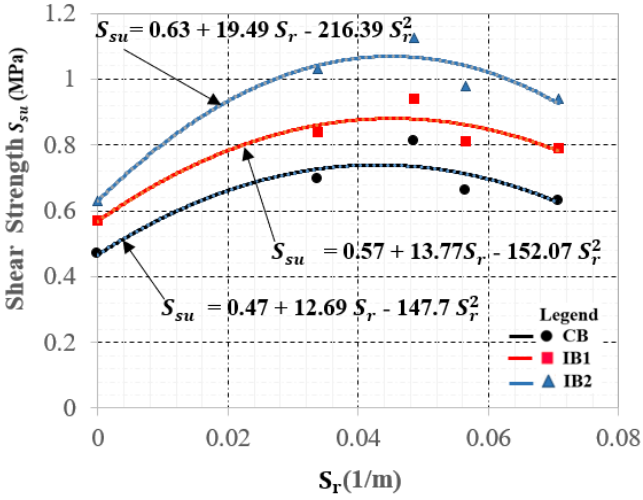

Fig. 22. Shear strength and specific surface of reinforcement for Diagonal Tension test.

A comparison between the maximum compressive strength of prism test obtained from this study and the other types of interlocking block from the previous studies are presented in Table 12. The results of the shear strength of diagonal test are shown in Table 13. The specimen CC1-W1 was produced from cement clay hollow brick. The specimens IBC-W and BLA-N1 were prepared with concrete block. When they are compared with the same density, the interlocking block in this study (IB2-P-CT) provided the compressive strength of 4.03 MPa and the shear strength of 0.63 MPa which were greater than those of IBC –W (1.45 MPa, 0.46 MPa), respectively. The effect of the saw tooth shear key

enhanced more strength than the straight shear key. For the different density, the specimen that possessed higher density (BLA-N1) provided greater compressive strength (7.02 MPa) than the interlocking block in this study (4.03 MPa). The higher density enhanced the strength of concrete block (f_b) resulting to the higher compressive strength of prism. It was observed that the specimen with the circular shear key provided comparable shear strength (0.62 MPa for CCI-W1) with that of the saw tooth shear key (0.63 MPa for IB2-DT-CT).

Table 12. Comparison of prism test results.

Test results	Specimen	Density (T/m^3)	f_b (MPa)	f'_m (MPa)
M.Teguh et al. [32]	IBC -W	1.60	-	1.45
E.H.Fahmy [33]	BL.A-N1	2.14	13.22	7.02
This study	IB2-P-CT	1.60	5.00	4.03

Table 13. Comparison of diagonal test results.

Test results	Specimen	Density (T/m^3)	f_b (MPa)	S_{su} (MPa)
M.Teguh et al. [32]	IBC-W	1.60	-	0.46
P. Joyklad [7]	CCI-W1	1.80	6.74	0.62
This study	IB2-DT-CT	1.60	5.00	0.63

(Remark: f_b is the compressive strength of interlocking block alone)

4. Conclusions

The lightweight concrete interlocking block panel was developed with water treatment sludge and expanded metal ferrocement. The conclusions can be drawn as follows:

a) The water treatment sludge is suitable for producing the concrete block with the sludge and fine aggregate ratio of 0.3. The optimum sludge content of 30% provided the compressive strength of 12.98 Mpa, the density of 1.63 Ton/m^3 and the water absorption of 15.92% conforming to the lightweight concrete block according to the Thai Industrial Standard.

b) The strength and ductility of specimens with expanded metal are greater than that of the conventional wire meshed for all types of concrete blocks. The effects of mesh type with overlapped diamond shape of the expanded metal contributed the strength and ductility that is superior to the conventional wire mesh.

c) Among the expanded metal mesh, for the small meshes, the high value of S_r enhanced the bond strength between the mesh and the block panel resulting to the high compressive strength of prism. For the case of large meshes, debonding occurred under loading. The large meshes could not achieve their load carrying capacity corresponding to their mesh sizes. Additional investigation is required for further study to improve the efficiency of expanded metal mesh such as the strengthening with the addition of tightened bolts

d) The effect of shear key for interlocking block enhanced the bond strength between each concrete block when compared to the conventional block. However, the contribution of shear key for the interlocking block significantly affected to the ductility capacity rather than the strength.

e) Among the different construction types of shear key, the shear key with thick bed cement mortar is more effective than the thin bed adhesive mortar typically used in the construction of lightweight concrete. The compressive strength of IB2-P was significantly enhanced due to the high adhesive strength of cement mortar with thick bed improved the bond strength transmitted by the shear key between each interlocking block.

f) Among the control specimens of diagonal tension test, the shear strength of the interlocking block IB1 and IB2 were enhanced by 21%, 34%, respectively compared to the conventional concrete block. This indicated that the use of shear key for interlocking block could improve the shear strength of the concrete block

g) It is evidenced that the ultimate shear strength (S_{su}) and the modulus of rigidity (G) of all types of the strengthened specimens are greater than that of the control specimen. Among the strengthened specimens IB1-DT and IB2-DT, the strengthened interlocking blocks (IB2-DT) was superior to that of IB1-DT. For the shear strength, the shear key with thick bed cement mortar is more effective than the thin bed adhesive mortar typically used in the construction of lightweight concrete.

Acknowledgement

This research is partly supported by V & P Expanded Metal. The authors appreciated for kind assistance of the laboratory staffs in the Civil Engineering Department, Sripatum University.

References

[1] S. B. Kadam, Y. Singh, B. Li. "Strengthening of unreinforced masonry using welded wire mesh micro-concrete – Behaviour under in-plane action," *Construction and Building Materials*, vol. 54, pp. 247–257, 2014.

[2] A. Leeanansaksiri, P. Panyakapo, and A. Ruangrassamee, "Seismic capacity of masonry infilled RC frame strengthening with expanded metal ferrocement, *Engineering Structures*," vol. 159, pp.110-127, 2018.

[3] S. Longthong, P. Panyakapo, and A. Ruangrassamee, "Seismic strengthening of RC frame and brick infill panel using ferrocement and expanded metal," *Engineering Journal*, vol. 24, no. 3, pp. 45-59, 2020.

[4] M. Ali, R. J. Gultom, and N. Chouw, "Capacity of innovative interlocking blocks under monotonic loading," *Construction and Building Materials*, vol. 37 pp. 812–821, 2012.

[5] Z. Tang, M. Ali, and N. Chouw, "Residual compressive and shear strengths of novel coconut-fibre-reinforced-concrete interlocking blocks," *Construction and Building Materials*, vol. 66, pp. 533–540, 2014.

[6] P. Joyklad, Q. Hussain, and N. Ali, "Mechanical properties of cement-clay interlocking (CCI) hollow bricks," *Engineering Journal*, vol. 24, no. 3, pp. 89-106, 2020.

[7] P. Joyklad and Q. Hussain, "Performance of cement clay interlocking hollow brick masonry walls subjected to diagonal compression," *Journal of Engineering Science and Technology*, vol. 14, no. 4, pp. 2152 – 2170, 2019.

[8] P. Joyklad and Q. Hussain, "Axial compressive response of grouted cement–clay interlocking hollow brick walls," *Asian Journal of Civil Engineering*, vol. 20, pp. 733-744, 2019.

[9] Q. Afzal, S. Abbas, W. Abbass, A. Ahmed, R. Azam, and M. R. Riaz, "Characterization of sustainable interlocking burnt clay brick wall panels: An alternative to conventional bricks," *Construction and Building Materials*, vol. 231, pp. 117190-117200, 2020.

[10] C. Suksiripattanapong, S. Horpibulsuk, P. Chanprasert, P. Sukmak, and A. Arulrajah, "Compressive strength development in fly ash geopolymer masonry units manufactured from water treatment sludge," *Construction and Building Materials*, vol. 82, pp. 20–30, 2015.

[11] C. Suksiripattanapong, S. Horpibulsuk, S. Boongrasan, A. Udomchai, A. Chinkulkijniwat, and A. Arulrajah, "Unit weight, strength and microstructure of a water treatment sludge–fly ash lightweight cellular geopolymer," *Construction and Building Materials,* vol. 94, pp. 807–816, 2015.

[12] R. K.Gomes, P. Edna, D. B. G. D. Santos, and C. Mauricio, "Potential uses of waste sludge in concrete production," *Management of Environmental Quality*, vol. 28, no. 6, pp. 821–838, 2017.

[13] Y. Liu, Y. Zhuge, C. W. Chow, A. Keegan, D. Li, P. N. Pham, J. Huang, and R. Siddique, "Utilization of drinking water treatment sludge in concrete paving blocks: Microstructural analysis, durability and leaching properties," *Journal of Environmental Management,* vol**.** 262, p. 110352, 2020.

[14] N. H. Rodríguez, S. M. Ramírez, M. B. Varela, M. Guillem, J. Puig, E. Larrotcha, and J. Flores. "Re-use of drinking water treatment plant (DWTP) sludge: Characterization and technological behaviour of cement mortars with atomized sludge additions," *Cement and Concrete Research*, vol. 40, no. 5, pp. 778–786, 2010.

[15] M. Alqam, A. Jamrah, and H. Daghlas, "Utilization of cement incorporated with water treatment sludge," *Jordan Journal of Civil Engineering*, vol. 5, pp. 268–277, 2011.

[16] S. H. Al-Tersawy and F. A. El Sergany, "Reuse of water treatment plant sludge and rice husk ash in concrete production" *International Journal of Engineering Science & Research Technology*, vol. 5, no.12, pp. 138–152, 2016.

[17] T. Ahmad, K. Ahmad, M. Alam. "Investigating calcined filter backwash solids as supplementary cementitious material for recycling in construction practices," *Construction and Building Materials*. vol.175, pp. 664–671, 2018.

[18] L.G.G. Godoy, A.B. Rohden, M.R. Garcez, S. Dalt, L.B. Gomes. Production of supplementary cementitious material as a sustainable management strategy for water treatment sludge waste. *Case Studies in construction Materials*, vol.12: e00329, 2020.

[19] C. Huang and S. Wang. "Application of water treatment sludge in the manufacturing of lightweight aggregate," *Construction and Building Materials*. vol. 43, pp. 174-183, 2013.

[20] A. Sales, F.R. Souza, W.R. Santos, A.M. Zimer, and F.C.R. Almeida, "Lightweight composite concrete produced with water treatment sludge and sawdust: Thermal properties and potential application," *Construction and Building Materials*. vol. 24, pp. 2446-2453, 2010.

[21] A. Sales, F. R. Souza, and F. C. R. Almeida. "Mechanical properties of concrete produced with a composite of water treatment sludge and sawdust," *Construction and Building Materials,* vol. 25, pp. 2793–2798, 2011.

[22] *Standard Specification for Concrete Aggregates*, ASTM Standard No. ASTM C 33-18, American Society for Testing Materials (ASTM), 2018.

[23] *Expanded Metal Standard by Japanese Industrial Standard,* JIS Standard No. JIS G3351, Japanese Standards Association, 1987.

[24] *Standard for Aerated Lightweight Concrete Block*, TIS 2601-13, Thai Industrial Standard (TIS), Department of Industrial Product Standard, Ministry of Industry, Thailand, 2013.

[25] *Standard Test Method for Compressive Strength of Hydraulic Cement Mortars*, ASTM Standard No. ASTM C 109/C 109M-02, American Society for Testing Materials (ASTM), 2002.

[26] *Standard Test Method for Density, Absorption, and Voids in Hardened Concrete,* ASTM Standard No. ASTM C642-97, American Society for Testing Materials (ASTM), 1997.

[27] *Standard Test Method for Compressive Strength of Masonry Prisms*, ASTM Standard No. ASTM C1314-07, American Society for Testing and Materials (ASTM), 2007.

[28] *Standard Test Method for Diagonal Tension (Shear) in Masonry Assemblages*, ASTM Standard No. ASTM E519-02, American Society for Testing and Materials (ASTM), 2002.

[29] *Standard for Sampling and Testing Concrete Masonry Units*, TIS 109-74, Thai Industrial Standard (TIS), Department of Industrial Product Standard, Ministry of Industry, Thailand, 1974.

[30] *Standard for Hollow Non-Load-Bearing Concrete Masonry Units*, TIS 58-87, Thai Industrial Standard (TIS),

Department of Industrial Product Standard, Ministry of Industry, Thailand, 1987.
[31] P. Panyakapo, "Cyclic pushover analysis procedure to estimate seismic demands for buildings," *Engineering Structures,* vol. 66, pp. 10-23, 2014.
[32] M. Teguh, F. W. Rivai, N. Rahmyanti, and E. W. Pradana, "Experimental investigation on interlocking concrete block for masonry wall of non-engineered earthquake resistant buildings," in *E3S Web of Conferences* 156, 05016, 2020, 4th ICEEDM 2019.
[33] E. H. Farmy and T.G.M. Ghoneim, "Behaviour of concrete block masonry prisms under axial compression," *Canadian Journal of Civil Engineering*, vol. 22, pp. 898-915, 1995.

Rattawit Amornpunyapat received the B.Eng. degree in Civil Engineering from Kasembundit University, Bangkok, Thailand in 1997.

He has worked in the construction industry as a civil engineer since 1997. His experience involves the construction of buildings and infrastructures. Since 2015, he has been a student in Master of Engineering Program in Civil Engineering, Sripatum University. His research interests include seismic strengthenening of buildings.

Phaiboon Panyakapo received the B.Eng. degree in Civil Engineering from Kasertsart University, Bangkok, Thailand in 1982 and the M.Eng. and D.Eng. degrees in Structural Engineering from Asian Institute of Technology, Pathumthani, Thailand, in 1984 and 1999.

From 1997- present, he has worked at Department of Civil Engineering, School of Engineering, Sripatum University. Since 2004, he has been an Associate Professor at the Civil Engineering Department, Sripatum University, Bangkok, Thailand. He is the author of three books, more than 20 articles, and 1 invention (in patent process). His research interests include building design, seismic design, precasted concrete design, performance based design and seismic retrofit of buildings. He is an Associate Editor of the journal, Sripatum Review of Science and Technology.

Mallika Panyakapo received the B.Sc. degree in Chemistry from Chulalongkorn University, Bangkok, Thailand in 1984 and the M.Sc. degree in Environmental science from Kasertsart University, Bangkok, Thailand in 1987 and D.Tech.Sc. degrees in Environmental engineering from Asian Institute of Technology, Pathumthani, Thailand, in 1997.

From 1987 - present, she has worked as a lecturer at Department of Environmental Science, Faculty of Science, Silpakorn University. Since 2008, she has been an Associate Professor in Environmental Science area. She is the author of three books and more than 20 articles. Her research interests include waste utilization, water and wastewater treatment and environmental management.